Electrochimica Acta 56 (2011) 4281–4286

Contents lists available at ScienceDirect

Electrochimica Acta

journal homepage: www.elsevier.com/locate/electacta

Electrochromic properties of porous NiO thin film as a counter electrode for NiO/WO_3 complementary electrochromic window

H. Huang[a], J. Tian[a], W.K. Zhang[a,*], Y.P. Gan[a], X.Y. Tao[a], X.H. Xia[b], J.P. Tu[b]

[a] College of Chemical Engineering and Materials Science, Zhejiang University of Technology, Hangzhou 310014, China
[b] Department of Materials Science and Engineering, Zhejiang University, Hangzhou 310027, China

ARTICLE INFO

Article history:
Received 27 August 2010
Received in revised form 18 January 2011
Accepted 22 January 2011
Available online 28 January 2011

Keywords:
Nickel oxide
Electrochromism
Thin film
Electrochromic window
Lithium intercalation

ABSTRACT

Highly porous nickel oxide (NiO) thin films were prepared on ITO glass by chemical bath deposition (CBD) method. SEM results show that the as-deposited NiO film is constructed by many interconnected nanoflakes with a thickness of about 20 nm. The electrochromic properties of the NiO film were investigated in a nonaqueous $LiClO_4$–PC electrolyte by means of optical transmittance, cyclic voltammetry (CV) and electrochemical impedance spectroscopy (EIS) measurements. The NiO film exhibits a noticeable electrochromic performance with a variation of transmittance up to 38.6% at 550 nm. The CV and EIS measurements reveal that the NiO film has high electrochemical reaction activity and reversibility due to its highly porous structure. The electrochromic (EC) window based on complementary WO_3/NiO structure shows an optical modulation of 83.7% at 550 nm, much higher than that of single WO_3 film (65.5% at 550 nm). The response time of the EC widow is found to be about 1.76 s for coloration and 1.54 s for bleaching, respectively. These advantages such as large optical modulation, fast switch speed and excellent cycle durability make it attractive for a practical application.

1. Introduction

Electrochromic (EC) materials are able to change their optical properties reversibly and persistently by an external voltage. The transition metal oxide thin films, e.g. oxides of W, Ir, V, Ti and Ni [1–4], are widely studied for their electrochromic behavior. Among these materials, NiO is of considerable interest due to high coloration efficiency (CE), good cyclic reversibility and low material cost [5,6]. In the past years, many studies on the electrochemical and electrochromic properties of NiO have been conduced in aqueous electrolytes, where the optical modulation depends on proton/electron transport [7–10]. Additionally, the electrochromic effect during the injection/extraction of Li^+ in/from NiO films has been observed in water-free organic system [11–14]. Considering practical applications, high coloration efficiency and long-term durability are required for NiO film. Therefore, nonaqueous organic solvents are more suitable as the electrolyte solution in comparison with aqueous electrolyte solution because the nonaqueous electrolyte has a wider potential window for electrochemical reactions. However, there are a few reports on the electrochromism and electrochemical performance of NiO films in nonaqueous electrolyte solutions [15,16].

A high performance EC device should present high optical contrast, good optical memory and chemical stability to electrochromic cycles. NiO films are being developed for application in dynamic or "smart" windows that are at the forefront of emerging energy-saving advances in building technologies [17]. NiO can be used as a counter electrode to WO_3 electrode in EC window, where the optical modulation increases because they are quite complementary [18,19]. However, in the fabricating process of EC window, they are chemically incompatible when NiO and WO_3 have to be immersed in acidic or alkaline aqueous electrolytes. The aqueous electrolyte can be replaced by nonaqueous solvents such as propylene carbonate (PC) and γ-butyrolactone. It has been revealed that WO_3 has a very reversible electrochromic behavior in the cited $LiClO_4$–PC electrolyte [20–22]. The use of WO_3 as the primary electrode in EC window requires a counter electrode, which is reversible and electrochromic in a complementary mode. The porous structure of NiO film is believed to be helpful to the enhancement of electrochromic performance. In our previous work, we found that the NiO film prepared by chemical bath deposition (CBD) method had highly porous structure and exhibited excellent EC properties in KOH electrolyte [23]. However, to the best of our knowledge, few investigations have been conducted in organic systems. In the present work, we employed a simple CBD method to prepared highly porous NiO film and investigated the EC properties of NiO films as the counter

---

* Corresponding author at: College of Chemical Engineering and Materials Science, Zhejiang University of Technology, Zone 6, Chaohui, Hangzhou, Zhejiang 310014, China. Tel.: +86 571 88320394; fax: +86 571 88320394.
E-mail address: msechem@zjut.edu.cn (W.K. Zhang).

0013-4686/$ – see front matter © 2011 Elsevier Ltd. All rights reserved.
doi:10.1016/j.electacta.2011.01.078

electrode of an EC window based on NiO/WO_3 complementary structure.

2. Experimental

The porous NiO film was prepared by a chemical bath deposition (CBD) method [24]. The solution for CBD was obtained by mixing 80 ml of 1 M nickel sulfate, 60 ml of 0.25 M potassium persulfate and 20 ml of aqueous ammonia (25–28% NH_3) in a 250 ml pyrex beaker at room temperature. Clean indium–tin oxide (ITO, sheet resistance 25 Ω/□, 4 cm × 5 cm in sizes)-coated glass substrates were masked with polyimide tape to prevent deposition on the nonconductive sides. The ITO samples were placed vertically in the freshly solution and kept at 20 °C for 10 min to deposit the precursor film under constant vigorous stirring. Then they were washed with deionized water. After removing the tape masks, the coated samples were dried at 75 °C and then annealed at different temperatures (300 °C, 400 °C and 500 °C) in air for 1.5 h.

The structure of the samples was examined by X-ray diffraction (XRD, philips PC-APD) using Cu K_α radiation. The surface morphology was observed using a scanning electron microscopy (SEM, HITACHI S-4700 Π). The electrochromic properties were evaluated by UV–visible absorption spectra, which was measured on a spectrophotometer (UV-2550, SHIMADZU) equipped with an integrating sphere.

The characteristics of the electrochromic processes were investigated by cyclic voltammetry (CV), and electrochemical impedance spectroscopy (EIS), which were carried out in a three-electrode system using a CHI650B electrochemical workstation. 1 M non-aqueous solution of $LiClO_4$ in propylene carbonate (PC) was employed as the electrolyte. A platinum foil was used as the counter electrode and Ag/AgCl as the reference electrode.

The EC window was realized by facing a activated nickel oxide ITO-coated glass electrode with a pristine tungsten oxide ITO-coated glass electrode in the $LiClO_4$–PC electrolyte. The WO_3 film used in this case was obtained by electrodeposition method [25,26]. The two-electrode window was assembled with epoxy glue in the dry box. The distance between the electrodes was 2.0 mm. The performances of the EC device were tested by double-potential-step experiment and by optical transmission spectra.

3. Results and discussion

Hydroxide precursor thin film was prepared using chemical bath deposition. The chemical reactions may occur as follows [27]:

$$[Ni(H_2O)_{6-x}(NH_3)_x]^{2+} + 2OH^- \rightarrow Ni(OH)_2 + (6-x)H_2O + xNH_3 \quad (1)$$

$$2Ni(OH)_2 + S_2O_8{}^{2-} \rightarrow 2NiOOH + 2SO_4{}^{2-} + 2H^+ \quad (2)$$

The XRD patterns of powders from the as-deposited precursor and annealed films on ITO substrate are presented in Fig. 1. All the peaks of pattern a in Fig. 1 indicate that the as-deposited precursor film contains β-$Ni(OH)_2$ (JCPDS 14-0117) and γ-NiOOH (JCPDS 06-0075). The typical peaks of cubic NiO phase (JCPDS 4-0835) can be found in Fig. 1(b–d), indicating that polycrystalline NiO films have formed after heat treatment. Although the XRD patterns of the NiO films annealed at 400 and 500 °C are similar to that of the film annealed at 300 °C, there is a slight difference, the relative intensities of the former are stronger than those of the latter. It indicates that higher annealing temperature is favorable to the formation of compact crystalline NiO.

Fig. 2 shows the SEM images of NiO films annealed at 300 °C, 400 °C and 500 °C. It can be seen that the morphologies of the films

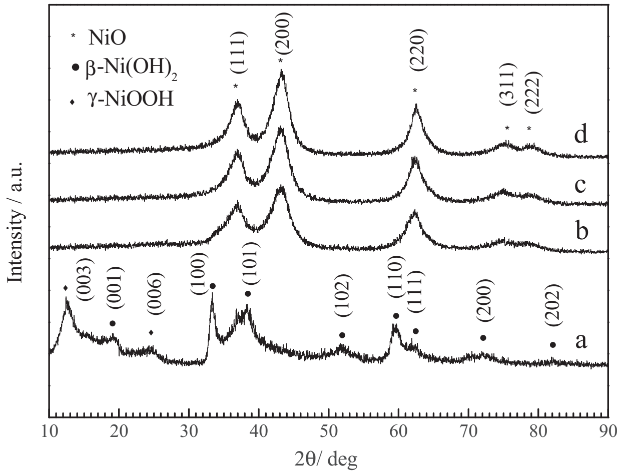

Fig. 1. XRD patterns of powders from the annealed films (a) as-deposited precursor film and the films annealed at (b) 300 °C, (c) 400 °C, (d) 500 °C.

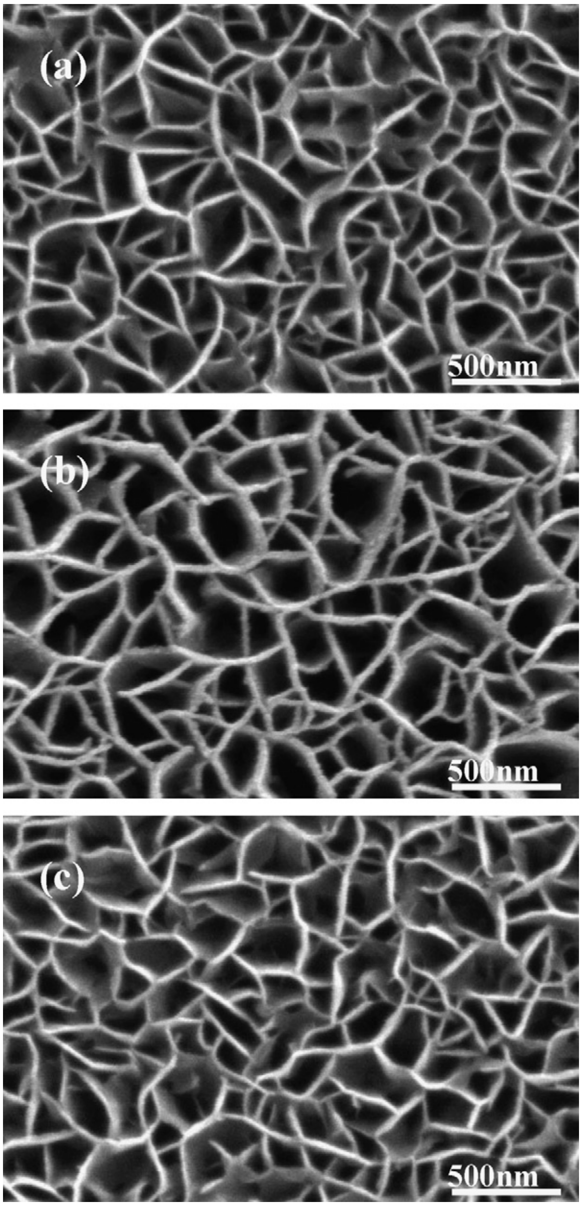

Fig. 2. SEM images of NiO films annealed at (a) 300 °C, (b) 400 °C and (c) 500 °C.

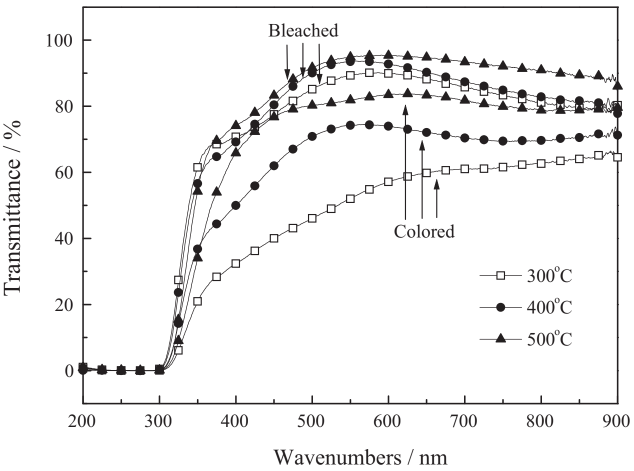

Fig. 3. Optical transmittance spectra of NiO thin films annealed at different temperatures.

have no distinctive differences after annealing at different temperatures. The NiO film is porous, and it is constructed by many interconnected NiO nanoflakes with a thickness of about 20 nm. These nanoflakes grow vertically on the substrate, forming a net-like structure and leaving pores with sizes of about 50–250 nm. It is generally believed that the highly porous structure will allow better penetration of electrolyte to promote lithium ions diffusion. During the electrode reaction, the diffusion length of lithium ions in the film is short, resulting in fast insertion/extraction reaction and thus obtaining good performance.

The electrochromic properties of the NiO films were measured after the film electrodes had been subjected to cyclic voltammetric test for 20 cycles in LiClO4–PC electrolyte. The NiO film electrodes were colored by applying a step potential of −1 V for coloration and −2 V (vs. Ag/AgCl) for bleaching. The color of the NiO film changes from brown black (colored state) to transparent (bleached state). Fig. 3 shows transmittance spectra of the annealed NiO films in the colored and bleached states. It clearly reveals that the transmittance variation decreases as the annealing temperature increases. The NiO film annealed at 300 °C presents the best electrochromic performance, the transmittance variation between colored and bleached states is high up to 38.6% at 550 nm, which is higher than that of the films annealed at 400 and 500 °C. The XRD results reveal that the high annealing temperature contributes to the formation of compact and well-crystallined NiO. This is in accord with the result obtained by Korošec et al. [28]. The electrochromic processes are associated with the double injection (extraction) of lithium ions and electrons into (from) the film. However, a fully crystalline film may be too dense for ions intercalation, and it will result in low electrochromic performance.

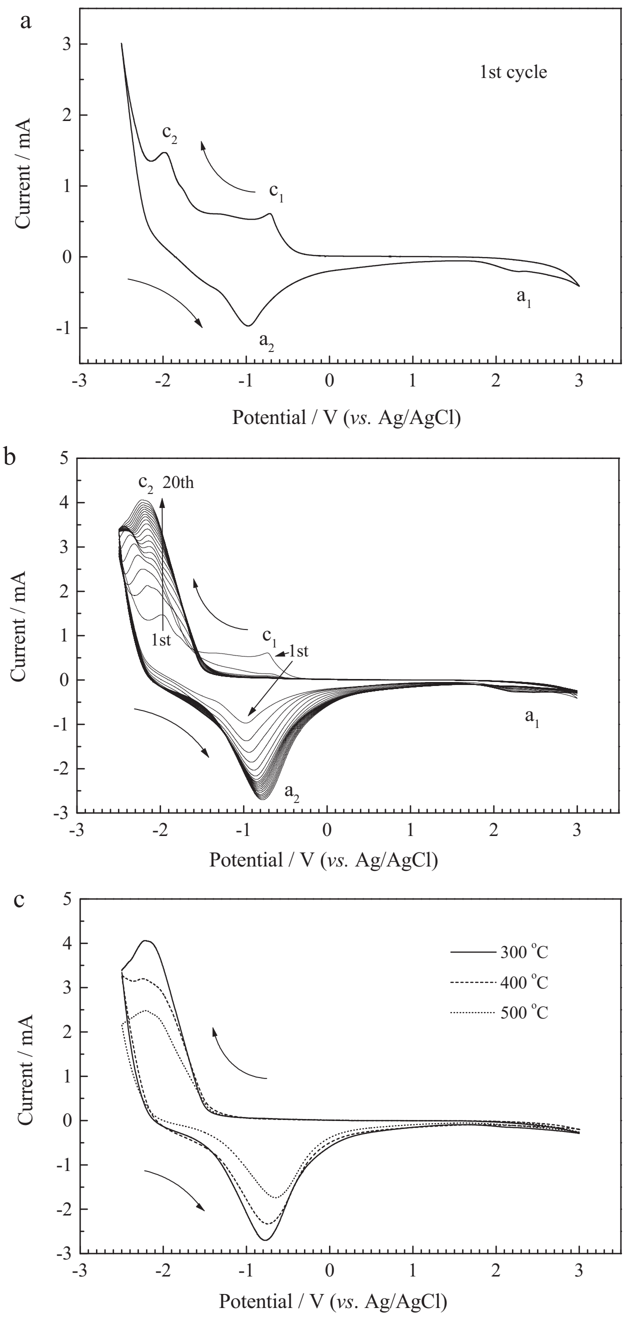

Fig. 4. Cyclic voltammograms of NiO thin films. Scan rate: 10 mV/s.

Fig. 4 shows the CV curves of NiO films in 1 M $LiClO_4$/PC electrolyte at a scan rate of 10 mV/s. In the first cycle of the NiO film annealed at 300 °C (Fig. 4(a)), two cathodic (insertion) peaks (c_1, c_2) at −0.72 and −1.98 V can be found in the CV curve, meanwhile, two anodic (extraction) peaks (a_1, a_2) located at +2.26 and −1.04 V are observed, respectively. In the subsequent cycles as shown in Fig. 4(b), the c_1/a_1 peaks gradually disappear, however, the c_2/a_2 peak currents increase with an increase in the number of cycles, implying that the pair of c_2/a_2 peaks is highly reversible and the reaction activity of the NiO film increases with cycling. After the 20th cycle, the peak potentials and curve shape remain virtually unchanged. It has been reported that the c_1 cathodic peak corresponds to an initial and irreversible intercalation of lithium ions, which may activate the electrode by somewhat widening the host structures, favoring further and reversible lithium intercalation [12]. The simplified electrochemical reaction can be expressed as the following:

$$\mathrm{NiO} + y\mathrm{Li}^{+} + y\mathrm{e}^{-} \rightarrow \mathrm{Li}_{y}\mathrm{NiO} \tag{3}$$

The reproducible c_2/a_2 redox peaks can be ascribed to a fast and reversible insertion and extraction process of lithium ions:

$$\underset{\text{(colored)}}{\mathrm{Li}_{y}\mathrm{NiO}} + x\mathrm{Li}^{+} + x\mathrm{e}^{-} \rightarrow \underset{\text{(bleached)}}{\mathrm{Li}_{(x+y)}\mathrm{NiO}} \tag{4}$$

which is accompanied by an electrochromic effect. Fig. 4(c) shows the 20th CV curves of the NiO films annealed at 300 °C, 400 °C and 500 °C, respectively. The cathodic and anodic peak currents of the NiO film annealed at 300 °C are much higher than those of the NiO film annealed at 400 °C and 500 °C. Moreover, the anodic peak potential of the NiO film annealed at 300 °C moves slightly to lower direction in comparison with the other samples, leading

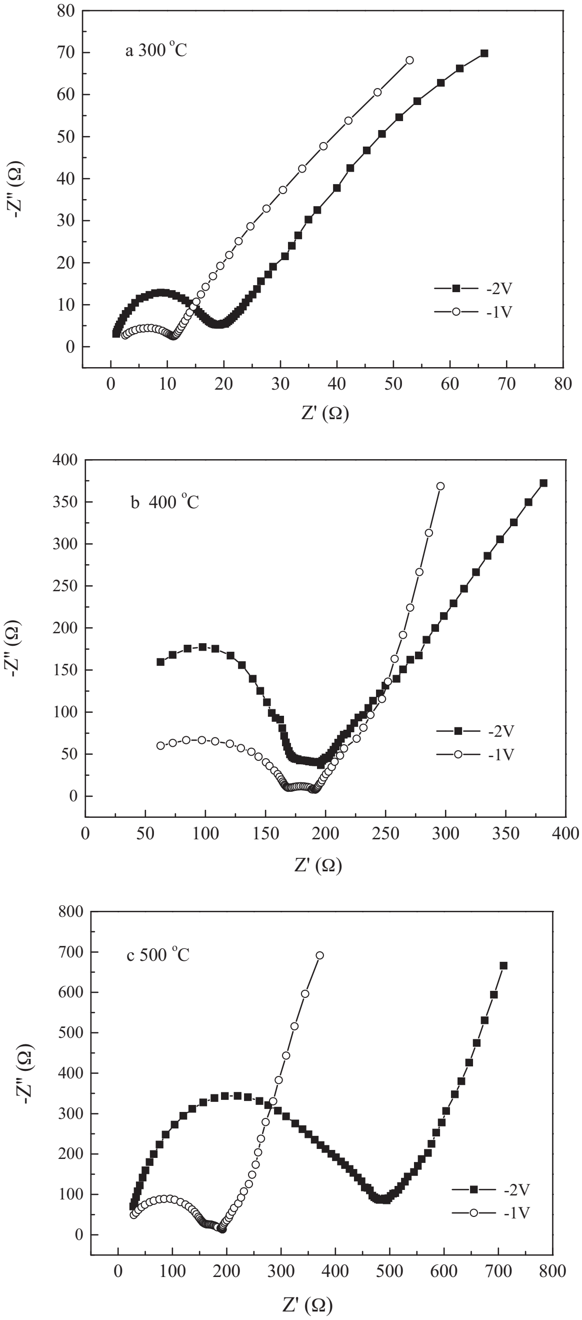

Fig. 5. Electrochemical impedance spectroscopy (EIS) of NiO film electrodes recorded at the peak potentials of −2 V and −1 V, respectively.

to a smaller potential separation between the oxidation peak and the reduction peak. It is well-known that the peak potential separation is used as a measure of reversibility. It indicates that the NiO film annealed at 300 °C has high electrochemical reversibility and activity, which is believed to be responsible for the superior electrochromic performance.

Fig. 5 shows the EIS of NiO film electrodes annealed at 300 °C, 400 °C and 500 °C. The EIS plots were recorded at the redox peak potentials of −2 V and −1 V, which corresponds to the insertion (extraction) processes of lithium ions, respectively. The EIS is composed of a depressed semicircle in the high frequency region and a sloping line in the low frequency region. Generally, the semicircle represents the charge-transfer resistance and the sloping line with a 45° angle is attributed to the diffusion of lithium ions into the bulk of electrode material. It can be seen that the NiO film annealed at 300 °C exhibits much smaller semicircle in the high frequency region and lower slope in the low frequency region, compared to those annealed at 400 °C and 500 °C. According to former reports [29], the smaller semicircle means the lower charge-transfer resistance, and the lower slope signifies the higher diffusion rate. It can be concluded that the NiO film annealed at 300 °C has the high charge-transfer rate and ion diffusion rate for lithium ion insertion and extraction.

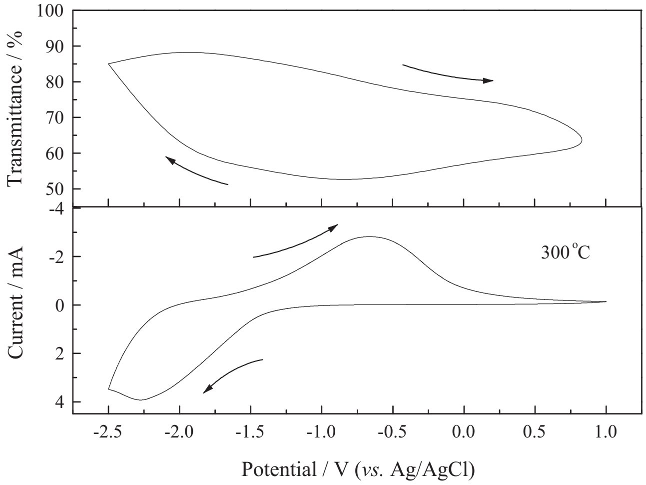

Fig. 6. Cyclic voltammogram (bottom) and in situ optical transmittance (top) of the NiO thin film annealed at 300 °C. Scan rate: 10 mV s^{-1}.

Fig. 6 shows the cyclic voltammertry and in situ transmittance of the NiO film annealed at 300 °C. The transmittance was measured at the wavelength of 550 nm. During the cathodic scan, the NiO film is almost transparent and the transmittance increases, while in the following anodic scan, the film gradually becomes brown black and the transmittance decays. The film shows good and repetitive optical response, as well as the fast switching time, which is very important for the realization of efficient EC window based on the WO_3 as main electrochromic material. The highly porous structure of NiO film facilitates electrolyte penetrating into the particles and shortens the ions diffusion path within the bulk of nickel oxide. Meanwhile, the intercrossing network provides much more paths for the double injection (extraction) of ions and electrons to (from) the film. All these contribute to the improvement of optical and electrochromic performances. These properties make lithiated NiO film of consistent interest for the realization of efficient EC window.

Commonly, the EC window use WO_3 as the main electrochromic electrode. Fig. 7 shows optical transmittance spectra of the WO_3 film at the 10th and 1000th cycle. The electrode was colored by applying a step potential of −1 V for 10 s and bleached by a potential of +2 V (vs. Ag/AgCl) for 10 s, respectively. The color of the WO_3 film changes from blue (colored state) to near transparent (bleached state). From Fig. 7, it can be seen that the optical transmittance of the WO_3 film is 87.6% in the bleached state and 22.1% in the colored state at 550 nm. The transmittance variation is about 65.5%, implying that the WO_3 has good electrochromic properties. Moreover, there is no significant difference in the transmittance between the 10th and 1000th cycle, indicating that the WO_3 film shows highly reversible electrochromic reaction and is suitable for EC window applications. Fig. 8 shows optical transmittance spectra of the EC window based on WO_3/NiO complementary structure applied at +2 V and −2 V for 10 s in the 10th and 1000th cycle, respectively. The transmittance variation of the EC window reaches about 83.7% at 550 nm, which is much higher than the single WO_3 film. The

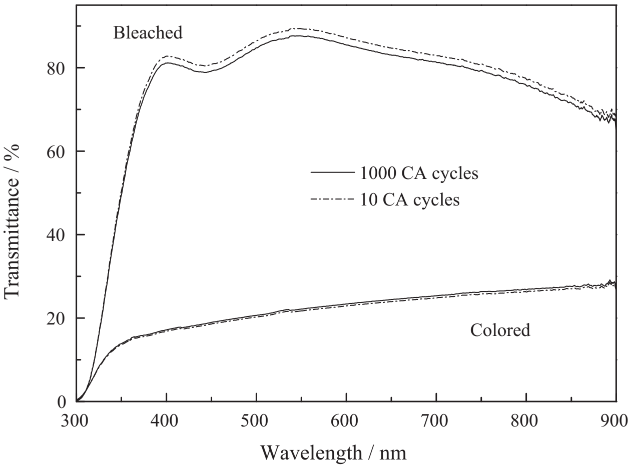

Fig. 7. Optical transmittance spectra of the WO_3 films in the colored and bleached states.

transmittance of EC window in the bleached state is similar to that of single WO_3 film (90.1% at 550 nm), however in the colored state, the transmittance of EC window is as low as 7.0% at 550 nm. Obviously, the improved electrochromic performance of EC window is attributed to the NiO layer. In addition, the optical transmittance of EC window has no obvious difference in the 10th and 1000th cycle, indicating that the EC window presents excellent reversibility and stability.

The switching speed from one state to another state and cycling stability of EC window is of great importance to determine its potential application. The time required for full bleaching from full colored state is defined as the response time. In this case, a double-potential-step cycling experiment was performed on the EC device (E_1 = 2.5 V, E_2 = −2.5 V), and the corresponding current–time response curves are shown in Fig. 9. From Fig. 9(a), it is concluded that the response time for coloration and bleaching is found to be about 1.76 and 1.54 s, respectively. The switching speed is much faster than the results reported by others [30,31]. Furthermore, the coloring current is almost the same as the bleaching current during the double-potential-step process and the current–time curves remain unchanged upon cycling. Indeed, the EC window based on complementary WO_3/NiO structure has efficient and reproducible behavior, since the current–time curves remain unchanged for many cycles (see Fig. 9(b)).

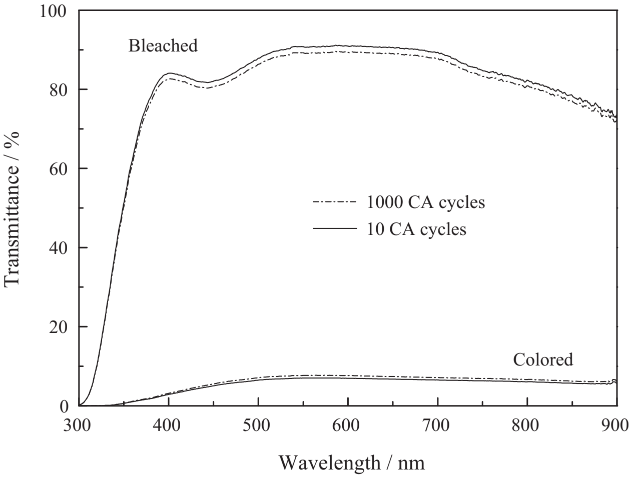

Fig. 8. Optical transmittance spectra of the EC window at the 10th and 1000th CA cycle.

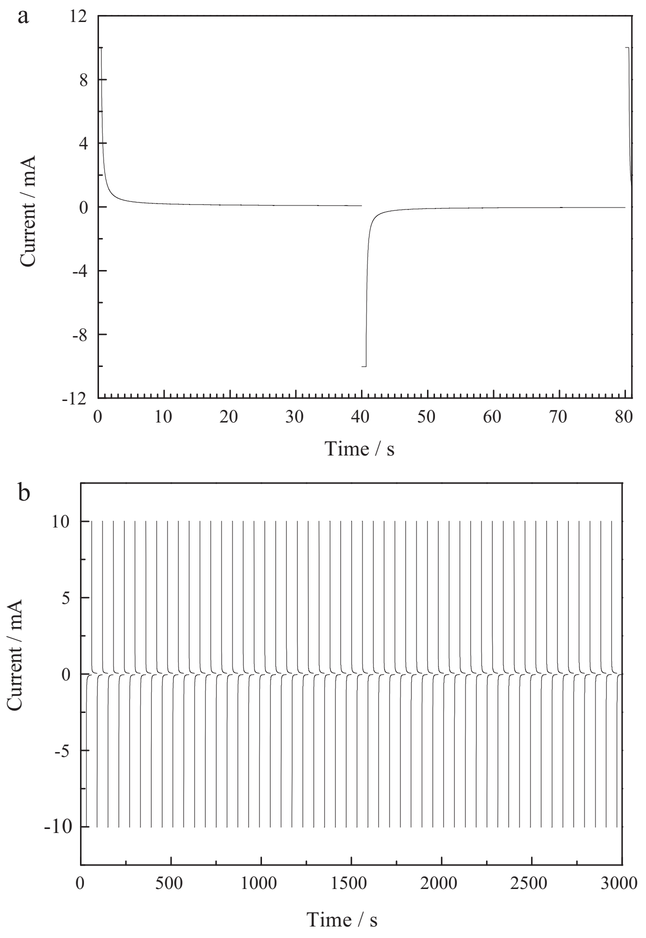

Fig. 9. Current–time response curves of the EC window during the double-potential-step cycling (a) 1 cycle (b) 50 cycles.

4. Conclusion

The NiO films with high porosity were prepared by a simple CBD method. XRD indicates that polycrystalline NiO films have been formed after annealing. SEM reveals a porous structure of NiO, which will allow better penetration of electrolyte to promote Li^+ ions diffusion and provide good electrochemical kinetics for injection/extraction of Li^+ ions. The NiO film annealed at 300 °C exhibits the best electrochromic performance with the variation of transmittance up to 38.6% at 550 nm. The assembled EC window based on WO_3/NiO complementary structure shows large optical modulation of 83.7% at 550 nm, much higher than that of single WO_3 film (65.5% at 550 nm), fast switch speed and excellent cycle durability, which make it very attractive for a practical application. The improved electrochromic performance of EC window is attributed to the NiO layer.

Acknowledgements

This work was supported by the National Natural Science Foundation of China (20673100 and 51002138), the 'Qianjiang Scholars' program of Zhejiang Province, the Natural Science Foundation of Zhejiang Province (Y4090420), the Qianjiang Project of Zhejiang Province (2010R10029).

References

[1] S. Green, J. Backholm, P. Georen, C.G. Granqvist, G.A. Niklasson, Sol. Energy Mater. Sol. Cells 93 (2009) 2050.

[2] G.A. Niklasson, C.G. Granqvist, J. Mater. Chem. 17 (2007) 127.
[3] H. Elzanowask, E. Miasek, V.I. Birss, Electrochim. Acta 53 (2008) 2706.
[4] S.Y. Kim, M. Taya, C.Y. Xu, J. Electrochem. Soc. 156 (2009) E40.
[5] T. Dutta, P. Gupta, A. Gupta, J. Narayan, J. Appl. Phys. 108 (2010) 083715.
[6] N.K. Shrestha, M. Yang, P. Schmuki, Electrochem. Solid-State Lett. 13 (2010) C21.
[7] X.H. Xia, J.P. Tu, J. Zhang, X.L. Wang, W.K. Zhang, H. Huang, Electrochim. Acta 53 (2008) 5721.
[8] S.A. Mahmoud, S.A. Aly, M. Abdel-Rahman, K. Abdel-Hady, Physica B 293 (2000) 152.
[9] H.R. Liu, W.M. Zheng, X. Yan, B.X. Feng, J. Alloys Compd. 462 (2008) 356.
[10] E.O. Zayim, I. Turhan, F.Z. Tepehan, N. Ozer, Sol. Energy Mater. Sol. Cells 92 (2008) 164.
[11] T. Kubo, Y. Nishikitani, Y. Sawai, H. Iwanaga, J. Electrochem. Soc. 156 (2009) H629.
[12] F. Decker, S. Passerini, R. Pileggi, B. Scrosati, Electrochim. Acta 37 (1992) 1033.
[13] A.C. Sonavanea, A.I. Inamdara, D.S. Dalavia, H.P. Deshmukhc, P.S. Patila, Electrochim. Acta 55 (2010) 2344.
[14] M. Li, A. Patra, Y. Sheynin, M. Bendikov, Adv. Mater. 21 (2009) 1707.
[15] E. Avendano, L. Berggren, G.A. Niklasson, C.G. Granqvist, A. Azens, Thin Solid Films 496 (2006) 30.
[16] T. Kubo, Y. Nishikitani, Y. Sawai, H. Iwanaga, Y. Sato, Y. Shigesato, J. Electrochem. Soc. 156 (2009) H629.
[17] T.G. Dane, C.T. Robert, C.D. Anne, J. Mater. Chem. 20 (2010) 9585.
[18] A. Subrahmanyam, C. Suresh Kumar, K. Muthu Karuppasamy, Sol. Energy Mater. Sol. Cells 91 (2007) 62.
[19] J. Zhang, J.P. Tu, X.H. Xia, Y. Qiao, Y. Lu, Sol. Energy Mater. Sol. Cells 93 (2009) 1840.
[20] M. Deepa, A.K. Srivastava, S.N. Sharma, Govind, S.M. Shivaprasad, Appl. Surf. Sci. 254 (2008) 2342.
[21] M. Deepa, A.G. Joshi, A.K. Srivastava, S.M. Shivaprasad, S.A. Agnihotry, J. Electrochem. Soc. 153 (2006) C365.
[22] M. Denesuk, J.P. Cronin, S.R. Kennedy, D.R. Uhlmann, J. Electrochem. Soc. 144 (1997) 1971.
[23] X.H. Xia, J.P. Tu, J. Zhang, X.L. Zhang, W.K. Zhang, H. Huang, Sol. Energy Mater. Sol. Cells 92 (2008) 628.
[24] H. Huang, L. Jiang, W.K. Zhang, Y.P. Gan, X.Y. Tao, H.F. Chen, Sol. Energy Mater. Sol. Cells 94 (2010) 355.
[25] K.J. Steveson, J.T. Hupp, Electrochem. Solid-State Lett. 2 (1999) 497.
[26] Y.S. Krasnov, G.Y. Kolbasov, Electrochim. Acta 49 (2004) 2425.
[27] S.Y. Han, D.H. Lee, Y.J. Chang, S.O. Ryu, T.J. Lee, C.H. Chang, J. Electrochem. Soc. 153 (2006) 382.
[28] R.C. Korošec, P. Bukovec, B. Pihlar, J.P. Gomilšek, Thermochim. Acta 402 (2003) 57.
[29] R.D. Armstrong, H. Wang, Electrochim. Acta 36 (1991) 759.
[30] F.L. Souza, M.A. Aegerter, E.R. Leite, Sol. Energy Mater. Sol. Cells 91 (2007) 1825.
[31] S.H. Lee, R. Deshpande, P.A. Parilla, K.M. Jones, B. To, A.H. Mahan, A.C. Dillon, Adv. Mater. 18 (2006) 763.